

Determination of the s -Electron Contact-Density Ratio for the Fe Configurations $3d^64s^2$ and $3d^64s$ from Matrix-Isolation Mössbauer Spectroscopy

H. Micklitz and F. J. Litterst

Physik-Department, Technische Universität München, 8046 Garching, West Germany

(Received 13 June 1974)

$^{57}\text{Fe}^+(3d^64s)$ ions have been produced by uv irradiation of a xenon matrix containing 0.65% ^{57}Fe . The stabilization of these ions was accomplished by mixing $\sim 1\%$ of HI into the Xe matrix gas. The Mössbauer isomer shift of the $^{57}\text{Fe}^+(3d^64s)$ resonance is $+0.26 \pm 0.03$ mm/sec against iron metal at 300 K. From this we obtain the ratio of the electron densities at the ^{57}Fe nucleus, $[\rho(0)_{3d^64s^2} - \rho(0)_{3d^6}]/[\rho(0)_{3d^64s} - \rho(0)_{3d^6}] = 1.80 \pm 0.15$.

Mössbauer studies of neutral atoms have been performed as absorption experiments using the rare-gas-matrix-isolation (RGMI) technique.¹ Mössbauer source experiments with RGMI $^{57}\text{Co}^{2+}$ and RGMI $^{119\text{m}}\text{Sn}^3$ extended these studies to charged ions ($^{57}\text{Fe}^+$ and $^{119}\text{Sn}^+$). The electronic configuration of these ions, however, depends on the specific recombination mechanism of the highly charged ions created by the Auger cascade following the radioactive decay. These ions are not stable against recombination with free electrons ($\tau_{\text{recomb}} \sim 3 \times 10^{-7}$ sec at 4.2 K).² A method for the production of these ions as stable species is of great interest, especially in connection with the problem of isomer-shift (IS) calibration. Stable ions then can be well specified and measured in absorption experiments.

We have generated and stabilized (for more than three weeks) $^{57}\text{Fe}^+(3d^64s)$ ions in a xenon matrix at ~ 4.5 K. The measured IS of this ion, together with the known IS of $^{57}\text{Fe}(3d^64s^2)$ and $^{57}\text{Fe}^{2+}(3d^6)$, gives an experimentally determined value for the ratio $\rho(0)_{4s^2}/\rho(0)_{4s}$ [here $\rho(0)$ is the difference in the relativistic electron density at the iron nucleus between the electron configuration given as the subscript and the $\text{Fe}^{2+}(3d^6)$ configuration]. This ratio is a sensible test for existing self-consistent-field (SCF) calculations of $\rho(0)$.

The generation and stabilization of the $^{57}\text{Fe}^+$ ions was accomplished by uv irradiation (wavelengths ~ 2500 – 3100 Å or photon energies ~ 4 – 5 eV) of a xenon matrix containing $(0.65 \pm 0.15)\%$ ^{57}Fe as electron donor and $\sim 1\%$ HI as electron acceptor. This method has already been used by Kasai⁴ for EPR studies of RGMI ions. Similar to Kasai we propose the following two-step process taking place during uv irradiation:

(1) Photodissociation of HI. HI shows continuous absorption between 2500 and 3100 Å leading to the $^3\Pi$ and $^1\Pi$ excited states of HI, which spon-

taneously dissociate into H and I^- .⁵

(2) Photoexcitation of Fe accompanied by a charge-transfer process between the excited Fe and the I atom: $\text{Fe}^* + \text{I}^- \rightarrow \text{Fe}^+ + \text{I}^-$. Fe atoms in a xenon matrix have six strong absorption bands between 2500 and 3100 Å leading to the different configurations of the excited states $3d^64s4p$ and $3d^74p$, respectively.⁶ The charge-transfer process probably occurs between the $3d^64s4p$ excited Fe states and the I^- state, since there is an energy resonance between these states [$E_{\text{ion}}(\text{Fe } 3d^64s4p) \sim E_{\text{ion}}(\text{I}^-)$]; such charge-transfer processes due to "energy resonance" between the two electronic levels involved have been reported earlier.^{2,7}

The resulting charged species Fe^+ and I^- should be separated by an average distance of ~ 20 Å. Such a separation is considered large enough that the influence of I^- on $\rho(0)$ of Fe^+ can be neglected provided both charged species are in their ground-state configuration.⁴ The electric field gradient (EFG) at the iron nucleus due to the splitting of the $\text{Fe}^+(^6D)$ state in the axial electric field of the I^- , however, is not negligible and will be discussed below.

The ^{57}Fe -doped Xe(HI) matrix was obtained by evaporating an iron foil ($\sim 80\%$ enriched ^{57}Fe) out of an alumina crucible, and mixing the iron atomic beam with a stream of Xe gas containing $\sim 1\%$ HI. This mixture was condensed on a liquid-helium-cooled beryllium disk (~ 4.5 K). Deposition rates were determined as described elsewhere.⁸ In this way a Xe(HI) matrix with an iron atomic concentration of $(0.65 \pm 0.15)\%$ corresponding to an amount of 65 ± 15 $\mu\text{g}/\text{cm}^2$ ^{57}Fe or $\sim 6 \times 10^{17}$ ^{57}Fe atoms/ cm^2 was produced. For the uv irradiation of the matrix we used a 450-W high-pressure xenon lamp together with a filter combination consisting of an uv filter (Schott UG5) and a solution filter of $\text{NiSO}_4 \cdot 6\text{H}_2\text{O}$ (0.3 g/ml H_2O , 5 cm absorption length); this filter combination is transpar-

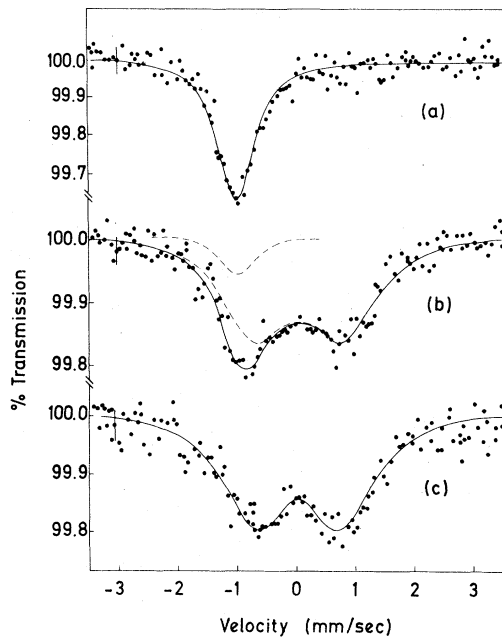


FIG. 1. Mössbauer absorption spectra of a xenon matrix containing $(0.65 \pm 0.15)\%$ ^{57}Fe ($65 \pm 15 \mu\text{g}/\text{cm}^2$ ^{57}Fe) and 1% HI. Matrix temperature ~ 4.5 K. Doppler velocities with respect to a $^{57}\text{Co}(\text{Cu})$ source at 300 K. (a) Spectrum before uv irradiation; (b) spectrum taken after ~ 5 h of uv irradiation; (c) spectrum taken after ~ 15 h of uv irradiation.

ent for wavelengths from 2500–3100 Å. The uv photon flux was $\sim 5 \times 10^{15} \text{ sec}^{-1} \text{ cm}^{-2}$ at the matrix.

Figure 1(a) shows the Mössbauer absorption spectrum of the ^{57}Fe -doped Xe(HI) matrix before uv irradiation. The spectrum shows a single resonance line (linewidth $\Gamma = 0.70 \pm 0.02 \text{ mm/sec}$) with an IS of $-0.74 \pm 0.02 \text{ mm/sec}$ with respect to iron metal at 300 K. This spectrum is identical with that found earlier for ^{57}Fe atoms in a Xe matrix without HI admixture.^{8,9} The Mössbauer absorption spectra taken after ~ 5 h ($\sim 10^{20}$ photons/ cm^2) and ~ 15 h ($\sim 3 \times 10^{20}$ photons/ cm^2) of uv irradiation are shown in Figs. 1(b) and 1(c), respectively. After ~ 5 h of uv irradiation a small fraction of the resonance line due to neutral $^{57}\text{Fe}(3d^6 4s^2)$ atoms can still be seen. After ~ 15 h of uv irradiation this resonance line is completely replaced by a quadrupole doublet with an IS of $0.26 \pm 0.03 \text{ mm/sec}$ against iron metal at 300 K and a splitting of $\Delta E_Q = 1.39 \pm 0.03 \text{ mm/sec}$.

We interpret the quadrupole doublet in Figs. 1(b) and 1(c) as the resonance of the charged $\text{Fe}^+(3d^6 4s)$ state. The quadrupole interaction is caused by the EFG of the $\text{Fe}^+(^6D)$ level split in

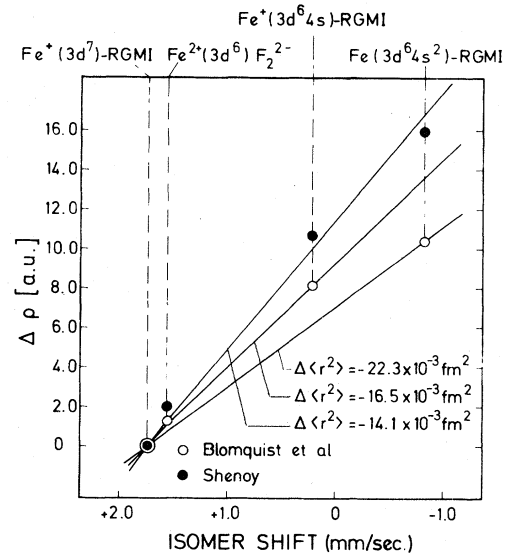


FIG. 2. Correlation between the relativistic electron density $\rho(0)$ at the ^{57}Fe nucleus and the isomer shift for ^{57}Fe . Isomer-shift values are given with respect to iron metal at 300 K. $\rho(0)$ values as calculated by Blomquist, Roos, and Sundbom, Ref. 11, and Shenoy, Ref. 13.

the axial electric field of a neighboring I^- . This splitting of the $\text{Fe}^+(^6D)$ level has been estimated to be $\sim 10 \text{ cm}^{-1}$ for an Fe^+-I^- distance of $\sim 20 \text{ \AA}$.¹⁰ The distribution of the Fe^+-I^- distances results in a variation of the $\text{Fe}^+(^6D)$ level splittings, and therefore in a distribution of the EFG at the iron nuclei. This is reflected in the large linewidth, $\Gamma = 1.42 \pm 0.02 \text{ mm/sec}$, of the quadrupole doublet.

Figure 2 shows a plot of the observed IS of RGMI $^{57}\text{Fe}(3d^6 4s^2)$, RGMI $^{57}\text{Fe}^+(3d^6 4s)$, and RGMI $^{57}\text{Fe}^+(3d^7)$ together with the IS of ^{57}Fe in FeF_2 versus the charge densities $\rho(0)$ of the corresponding configurations as calculated by Blomquist, Roos, and Sundbom¹¹ [nonrelativistic Hartree-Fock procedure corrected by a uniform relativistic enhancement factor $S'(Z) = 1.29$ ¹²] and as calculated by Shenoy¹³ (Dirac-Fock-Slater procedure). With the charge densities calculated by Shenoy the three RGMI "calibration" points of Fig. 2 are essentially consistent with a value of $\Delta\langle r^2 \rangle = -(14.1 \pm 0.7) \times 10^{-3} \text{ fm}^2$. This is not the case if we use the values obtained by Blomquist, Roos, and Sundbom. In this case one finds $\Delta\langle r^2 \rangle = -(22.3 \pm 0.5) \times 10^{-3} \text{ fm}^2$ from RGMI $\text{Fe}^+(3d^7)$ and RGMI $\text{Fe}(3d^6 4s^2)$ and $\Delta\langle r^2 \rangle = -(16.5 \pm 0.5) \times 10^{-3} \text{ fm}^2$ from RGMI $\text{Fe}^+(3d^7)$ and RGMI $\text{Fe}^+(3d^6 4s)$.

The $\Delta\langle r^2 \rangle$ value obtained from the $\rho(0)$ calculations by Shenoy is in agreement with those ob-

tained by Duff¹⁴ [$\Delta\langle r^2 \rangle = -(15.5 \pm 1.5) \times 10^{-3} \text{ fm}^2$] from a critical re-evaluation of the existing IS calibration attempts and by Kalvius and Shenoy¹⁵ [$\Delta\langle r^2 \rangle = -(15 \pm 5) \times 10^{-3} \text{ fm}^2$]. It also is in less disagreement with those obtained from measurements of the change in the lifetime of the 14.4-keV state in ⁵⁷Fe with the chemical environment: $\Delta\langle r^2 \rangle = -(8 \pm 1.5) \times 10^{-3} \text{ fm}^2$ ¹⁶ and $-(6 \pm 2) \times 10^{-3} \text{ fm}^2$.¹⁷

Effects of the rare-gas matrix on $\rho(0)_{4s^2}$ in the Fe($3d^6 4s^2$) atom seem to be $\lesssim 5\%$ as estimated from the observed IS differences of Fe atoms isolated in different inert matrices (Ar, Kr, Xe^{8,9}; N₂¹⁸; CH₄, CO₂¹⁹). Matrix effects on the spin density (hf-coupling constant) of RGMI Cu($3d^{10} 4s$) as measured by EPR experiments²⁰ are of the same order of magnitude ($\lesssim +5\%$). Matrix effects on RGMI ions can be estimated from EPR experiments with RGMI ions; the observed effects on the hf-coupling constant in Mn⁺($3d^5 4s$) and Cd⁺($4d^{10} 5s$) again are $\lesssim -5\%$.⁴ From these experimental facts we conclude that the rare-gas-matrix effects on $\rho(0)$ are $\lesssim \pm 5\%$ for all Fe configurations.

From the IS data of Fig. 2 we derive the ratio $[\rho(0)_{4s^2}/\rho(0)_{4s}]_{\text{exp}} = 1.80 \pm 0.15$. Taking into account possible influences of the rare-gas matrix, as discussed above, would lower this value by maximal 5%, that is, to $[\rho(0)_{4s^2}/\rho(0)_{4s}]_{\text{exp}} = 1.65 \pm 0.15$. This value is in good agreement with the calculations of Shenoy which give $[\rho(0)_{4s^2}/\rho(0)_{4s}]_{\text{calc}} = 1.6$. It is, however, in serious disagreement with the ratio $[\rho(0)_{4s^2}/\rho(0)_{4s}]_{\text{calc}} = 1.3$ as obtained by Blomquist, Roos, and Sundbom. From optical isotope-shift measurements on 6s- and 7s-electron configurations one finds $[\rho(0)_{ns^2}/\rho(0)_{ns}]_{\text{OIS}} = 1.6 \pm 0.1$ for $n = 6$ ²¹ and $n = 7$ ²² again in excellent agreement with our measured value for $n = 4$.

Therefore we come to the conclusion that the calculated value of Blomquist, Roos, and Sundbom for the Fe($3d^6 4s^2$) configuration is probably $\sim 35\%$ too low, i.e., the s shielding within the 4s shell seems to be overestimated in these calculations. This could be caused by the use of a single relativistic enhancement factor $S'(Z)$ for all Fe configurations despite the known fact that relativistic contributions to the shielding ratios can be important.²³

Our measurement shows that SCF calculations have to be treated with care. The relatively good agreement of our experimental data with

the Dirac-Fock-Slater calculations by Shenoy could be just fortuitous. More SCF calculations of ratios of charge densities of different iron configurations are needed. Their comparison with various density ratios from experiments provides a crucial test for the quality of such calculations.

We acknowledge helpful discussions with G. M. Kalvius, K. Luchner, G. K. Shenoy, and F. Wagner.

¹P. H. Barrett and H. Micklitz, in *Perspectives in Mössbauer Spectroscopy*, edited by S. G. Cohen and M. Pasternak (Plenum, New York, 1973), p. 117, and references contained therein.

²H. Micklitz and P. H. Barrett, *Phys. Rev. Lett.* **28**, 1547 (1972).

³H. Micklitz, P. H. Barrett, J. T. Waber, and H.-S. Kwoh, to be published.

⁴P. H. Kasai, *Phys. Rev. Lett.* **21**, 67 (1968).

⁵R. S. Mulliken, *Phys. Rev.* **51**, 310 (1937).

⁶D. M. Mann and H. P. Broida, *J. Chem. Phys.* **55**, 84 (1971).

⁷G. Gerth, K. Luchner, and H. Micklitz, *Phys. Status Solidi (b)* **53**, 593 (1972).

⁸T. K. McNab and P. H. Barrett, in *Mössbauer Effect Methodology* (Plenum, New York, 1971), Vol. 7, p. 59.

⁹T. K. McNab, H. Micklitz, and P. H. Barrett, *Phys. Rev. B* **4**, 3787 (1971).

¹⁰H. L. Schläefer and G. Gliemann, *Einführung in die Ligandenfeldtheorie* (Akademische Verlagsgesellschaft, Frankfurt, Germany, 1967), p. 351 ff.

¹¹J. Blomquist, B. Roos, and M. Sundbom, *J. Chem. Phys.* **55**, 141 (1971).

¹²D. A. Shirley, *Rev. Mod. Phys.* **36**, 339 (1964).

¹³G. K. Shenoy, private communication.

¹⁴K. J. Duff, *Phys. Rev. B* **9**, 66 (1974).

¹⁵G. M. Kalvius and G. K. Shenoy, to be published.

¹⁶R. Rueggsegger and W. Kuendig, *Phys. Lett.* **39B**, 620 (1972).

¹⁷R. N. Verma and G. T. Emery, *Phys. Rev. B* **9**, 3666 (1974).

¹⁸H. Micklitz and P. H. Barrett, *Appl. Phys. Lett.* **20**, 387 (1972).

¹⁹C. Klee, T. K. McNab, F. J. Litterst, and H. Micklitz, to be published.

²⁰P. H. Kasai and D. McLeod, *J. Chem. Phys.* **55**, 1566 (1971).

²¹H. Kopfermann, *Kernmomente* (Akademische Verlagsgesellschaft, Frankfurt, Germany, 1956), p. 164.

²²J. Blaise and A. Steudel, *Z. Phys.* **209**, 311 (1968).

²³M. A. Coulthard, *J. Phys. B: Proc. Phys. Soc.*, London **6**, 23 (1973).